

# Optimizing Material Strength Constants Numerically Extracted from Taylor Impact Data

by D. J. Allen, W. K. Rule and S. E. Jones

**ABSTRACT**—Advanced design requirements have dictated a need for the mechanical properties of materials at high strain rates. Mechanical testing for these data poses a significant problem for experimentalists. High-speed testing machines have a limited capability at rates approaching  $10^2/\text{s}$ . The split Hopkinson pressure bar is the most reliable alternative for rates approaching  $10^4/\text{s}$ . Plate impact experiments are capable of generating strain rates of  $10^8/\text{s}$  and higher. The Taylor impact test occupies a place of particular importance by providing data at strain rates on the order of  $10^4/\text{s}$ – $10^5/\text{s}$ . The issue at present is extracting the data. This paper provides a method for obtaining dynamic strength model material constants from a single Taylor impact test. A polynomial response surface is used to describe the volume difference (error) between the deformed specimen from the Taylor test and the results of a computer simulation. The volume difference can be minimized using an optimizer, with the result being an optimum set of material constants. This method was applied to the modified Johnson-Cook model for OFHC copper. Starting from a nominal set of material constants, the iterative process improved the relative volume difference from 23.1 percent to 4.5 percent. Other starting points were used that yielded similar results. The material constants were validated by comparing numerical results with Taylor tests of cylinders having varying aspect ratios, calibers and impact velocities.

## Introduction

The goal of this study was to develop a methodology to allow a single Taylor impact test to be used as a simple and cost-efficient means for obtaining and refining constants for dynamic material strength models. The majority of these models contain several material dependent constants. Normally, these constants are obtained by performing several complicated and sometimes costly experiments. The methodology presented here obtains the constants by minimizing the difference between the displacement results of a Taylor impact test and a hydrocode simulation of the event. The EPIC hydrocode was used for this study.<sup>1,2</sup>

EPIC treats plastic behavior by first assuming that stress increments are elastic and then correcting for cases where the equivalent (von Mises) stress  $\bar{\sigma}$  exceeds the local yield strength of the material  $\sigma_{\max}$  as given by the strength model. The correction simply involves scaling the local stress components by the factor  $\sigma_{\max}/\bar{\sigma}$ , thus forcing the stress state to

stay on the yield surface. Subsequent iterations ensure that equilibrium is maintained despite the stress corrections.

## Johnson-Cook Strength Model

The strength model used in this study was a modified form of the Johnson-Cook equation<sup>2,4</sup>

$$\sigma_{\max} = [A + B\epsilon^n] [\dot{\epsilon}^*]^C [1 - T^{*m}], \quad (1)$$

where  $\epsilon$  is the equivalent plastic strain and  $\dot{\epsilon}^* = \dot{\epsilon}/\dot{\epsilon}_0$  is the dimensionless plastic strain rate ( $\dot{\epsilon}_0 = 1.0 \text{ s}^{-1}$ ).  $T^*$  is the homologous temperature.  $A$ ,  $B$ ,  $n$ ,  $C$  and  $m$  are five empirical material constants.

This model was selected because it is widely used and accepted. It is one of several models available in EPIC. The form of the model was developed by observing how the strength of metals vary under different loading conditions, including a wide range of strains, strain rates and temperatures. Previously, test data for calibrating the strength model coefficients of different materials were produced using torsion tests over a range of strain rates, split Hopkinson pressure bar tests over a range of temperatures and quasi-static and dynamic uniaxial tension tests.

Many physically based alternatives to the modified Johnson-Cook strength model are available.<sup>5,6</sup> Strength models are continuously evolving in form and complexity.

## Taylor Impact Test

With material strength models becoming more complex, there is a need for simpler and more cost-efficient ways of obtaining material constants. One such way is by using the Taylor impact test. The Taylor impact test was performed in the 1940s by Sir Geoffrey Taylor<sup>7</sup> for the purpose of predicting the dynamic yield stress of materials subjected to high strain rates. The test consists of firing a cylinder at a flat, rigid target at speeds high enough to develop the strain rates of interest. His theory used the final deformed shape of the cylinder to determine a dynamic yield or flow stress of the material. Since then, Taylor's analytical theory has been modified by Lee and Tupper,<sup>8</sup> Hawkyard<sup>9</sup> and Jones, Gillis and Foster.<sup>10</sup>

Recently, the Taylor test has also been used to evaluate material strength models.<sup>3,5,11–13</sup> The computational results of hydrocodes using these models can be compared to the results of a Taylor test to evaluate the effectiveness of the model's form and the accuracy of its coefficients. This test

*D. J. Allen is a Graduate Student, W. K. Rule is Associate Professor and S. E. Jones is Professor, Department of Aerospace Engineering and Mechanics, University of Alabama, Box 870280, Tuscaloosa, AL 35487-0280.*

*Original manuscript submitted: September 23, 1996.*

*Final manuscript received: March 21, 1997.*

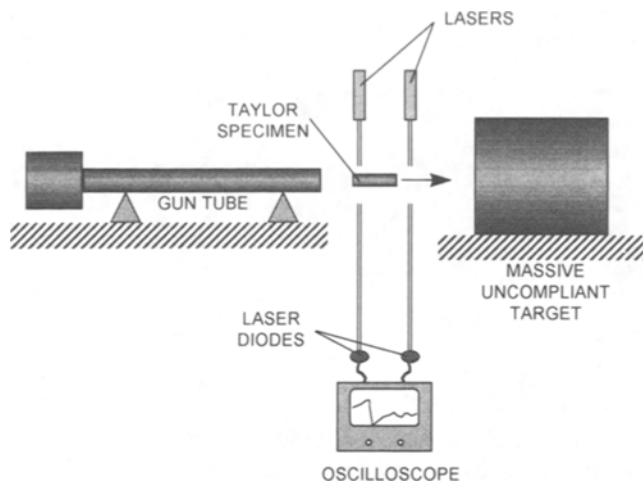


Fig. 1—Schematic drawing of Taylor test equipment

provides the high strains and strain rates necessary to evaluate the model independently of the tests used to obtain the material constants.

Until now, the Taylor test has rarely been used for obtaining constants for material strength models. Johnson and Holmquist<sup>14</sup> used the Taylor test to determine constants for both the Johnson-Cook and Zerilli-Armstrong models. Their method used only three dimensions from the deformed specimen (length, maximum diameter and an intermediate diameter) and was therefore only able to predict as many as three constants. The method to be presented here uses the entire profile and the length of the deformed specimen to determine the constants. For this reason, this method will theoretically be able to determine all constants in any given strength model.

The Taylor test setup used for this study is shown in Fig. 1 and is discussed in some detail by Allen.<sup>15</sup> OFHC (oxygen-free, high-conducting) copper was selected as the material for the impact specimen. OFHC copper is readily available, commonly used in high strain rate applications and can be easily machined into cylinders of the desired length and diameter. The primary specimen for use in the study was 7.87 mm in diameter, with an aspect ratio (length:diameter) of 5:1. This aspect ratio was chosen because specimens shorter than this do not usually display the complex curvature in the deformation profile that may be needed to uniquely determine model constants. With longer specimens, the greater mass can cause difficulties in achieving high velocities without fracturing the specimens.

The deformed lengths of the Taylor specimens were measured using calipers. The deformed profiles were measured using an optical comparator, which uses a light source to cast a magnified specimen shadow onto a viewing screen. The screen is divided into the desired units of measurement and scaled to the magnification used. Using the optical comparator, deformed profiles were measured to within  $\pm 0.03$  mm.

### Numerical Model for the Taylor Impact Specimen

A numerical model of a Taylor specimen requires specification of the following material properties: density; specific heat; initial, ambient, melting and absolute zero temperatures; and constants describing the strength model and the equation of state. The material properties used were ob-

TABLE 1—NOMINAL MATERIAL PROPERTIES OF OFHC<sup>a</sup> COPPER

Density (kg/m <sup>3</sup> )	8952
Specific heat (J/kg°C)	383.4
Specimen temperature (°C)	21.1
Melting temperature (°C)	1083
Modified Johnson-cook model constants	
Shear modulus (GPa)	46.3
A (MPa)	89.6
B (MPa)	291.6
n (dimensionless)	0.310
C (dimensionless)	0.025
m (dimensionless)	1.090
Mie-Grueneisen equation of state constants	
K <sub>1</sub> (GPa)	137.1
K <sub>2</sub> (GPa)	175.1
K <sub>3</sub> (GPa)	564.2
Γ (dimensionless)	1.960

a. OFHC = oxygen-free, high-conducting

tained from the material library included in EPIC. For this study, only the constants for the strength model were modified. The values of the OFHC copper properties used are given in Table 1.

The Taylor cylinder was modeled using three-node, triangular, axisymmetric, solid elements. For simplicity, the target was modeled as a rigid, frictionless surface. This has been the approach for numerically modeling the Taylor anvil in the past. It is assumed that the physical target is sufficiently rigid and free of friction to allow this approximation to be made.

### Mesh Refinement

A mesh refinement study was performed to determine the minimum number of nodes required to converge to a solution. The preprocessor in EPIC automatically generates the element mesh for an axisymmetric model by having the user input the number of element rings in the radial direction and the number of element layers in the longitudinal direction. The primary Taylor cylinder was modeled six different times with the number of element rings varying from 1 to 6. This gave a broad range of mesh densities, with the number of nodes varying from 32 to 787. The calculated deformed shapes produced by each of the six meshes were compared to measured results for a Taylor cylinder fired at 197 m/s. The comparison was based on the volume difference that will later be used to optimize the strength model constants. Because volume difference was the key index used for assessing the accuracy of the finite element results, it also provided a good index for mesh convergence and for determining the end of the impact event.

The volume difference is the sum of the longitudinal volume difference and the radial volume difference (which are based on profile and length discrepancies, respectively) between the physical test and the finite element model. Before determining the radial volume difference, the longitudinal dimensions of the finite element model were scaled such that its total length equaled that of the physical specimen. This was done to ensure that length discrepancies did not affect the calculation of the radial volume difference. For the physical specimen, the radius was measured every 0.51 mm along the entire length using the optical comparator. The finite el-

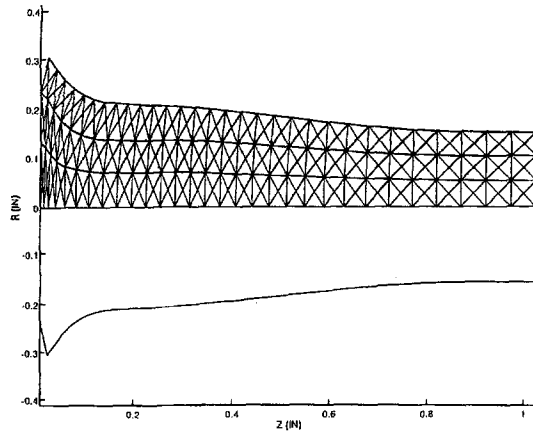


Fig. 2—Typical finite element mesh after impact

ement model's radius at each corresponding position was interpolated from a third-order polynomial fit through the four nearest profile node positions. For each 0.51-mm slice of the cylinder, the radial difference between the physical specimen profile and the finite element model profile forms a quadrilateral. The area of the quadrilateral was determined, and the volume of a ring generated by revolving this area around the longitudinal axis was calculated. The volume of this ring represents the volume difference associated with the 0.51-mm slice. The sum of the volume differences (always considered positive) for each of the slices represented the radial volume difference for the finite element model. When determining the longitudinal volume difference, it was assumed that there was essentially no plastic deformation toward the unimpacted end of the Taylor specimen. Accordingly, the longitudinal volume difference was given by the length difference between the measured and numerically modeled Taylor specimens times the undeformed cross-sectional area.

The results of the mesh refinement study are shown in Table 2. It can be seen that the mesh density did not seem to significantly affect the longitudinal volume difference for the models studied here. However, the radial volume difference, and hence the total volume difference, were greatly influenced by the mesh density. As the mesh density increased, the volume difference decreased until three element rings were reached, at which point the volume difference became essentially constant, indicating that the finite element solution reached convergence. Three element rings were used on all subsequent meshes. The effect of mesh density on computer runtime is also shown in Table 2. Figure 2 shows a typical deformed three-ring mesh.

### End of Event Test

A Taylor test simulation was run where the geometry data were output every 10  $\mu$ s, starting at 30  $\mu$ s and ending at 130  $\mu$ s. It was found that both the radial and longitudinal volume differences become essentially constant at approximately 100  $\mu$ s. Although this shows that the event ends at 100  $\mu$ s, for the remainder of the study, the simulation was allowed to run to 130  $\mu$ s to capture any end of event time variances due to altering the strength model constants.

### Determination of Strength Model Constants

The method presented here uses a complete second-order polynomial to describe how the volume difference varies with

changes in the strength model constants. The dimensionless polynomial used was of the following form:

$$\begin{aligned} V/V_0 = & 1 + \alpha_1 x_1 + \alpha_2 x_2 + \alpha_3 x_3 + \alpha_4 x_4 + \alpha_5 x_5 \\ & + \alpha_6 x_1 x_2 + \alpha_7 x_1 x_3 + \alpha_8 x_1 x_4 + \alpha_9 x_1 x_5 \\ & + \alpha_{10} x_2 x_3 + \alpha_{11} x_2 x_4 + \alpha_{12} x_2 x_5 + \alpha_{13} x_3 x_4 \\ & + \alpha_{14} x_3 x_5 + \alpha_{15} x_4 x_5 + \alpha_{16} x_1^2 + \alpha_{17} x_2^2 \\ & + \alpha_{18} x_3^2 + \alpha_{19} x_4^2 + \alpha_{20} x_5^2, \end{aligned} \quad (2)$$

where  $V$  is the volume difference and  $V_0$  is the baseline volume difference. The baseline volume difference is the volume difference that is obtained if the constants are not changed from their baseline values. The design variables  $x_i$  indicate percentage changes (from baseline) in the strength model constants, with  $x_1, x_2, x_3, x_4$  and  $x_5$  corresponding, respectively, to  $A, B, n, C$  and  $m$  of eq (1).

Equation (2) describes a  $p$ -dimensional response surface where  $p$  is equal to the number of strength model constants to be determined. Response surfaces are commonly used in optimization calculations to predict function behavior in the vicinity of known functional values. A complete second-order polynomial in  $p$ -dimensions requires  $q$  coefficients, where

$$q = 2p + \sum_{i=1}^p (i - 1). \quad (3)$$

For this study using eq (1),  $p = 5$  and thus  $q = 20$ , but these vary for models with differing numbers of strength model constants. A second-order polynomial was chosen because it can represent local minimums within the response surface. Higher order polynomials would more accurately describe the response surface but would require a great deal more data to determine the many additional polynomial coefficients.

To determine  $\alpha$  of eq. (2),  $q$  linearly independent values of  $V/V_0$  are needed. This required  $q$  EPIC runs using different strength model constants obtained by applying various combinations of  $x_i$  to span the  $p$ -dimensional space. Equation (2) is only valid in the vicinity of the baseline point and loses accuracy at points farther away. In this study, the variations on  $x_i$  used to determine  $\alpha$  were initially limited to  $\pm 10$  percent.

Knowing the baseline volume difference  $V_0$  and the coefficients of eq (2), the  $V/V_0$  ratio (and thus  $V$  the volume difference) can be minimized by varying  $x_i$ . This was conveniently accomplished using a spreadsheet function (the Solver tool of Microsoft® Excel®). Of course, other optimization routines could also be used for this purpose. The set of  $x_i$  determined by the optimizer serves as the initial point on the response surface for the next iteration of the solution process.

To start each iteration, the newest volume difference data point (as selected by the optimizer at the end of the previous iteration) was incorporated into eq (2) to define a new set of  $\alpha$ . One old volume difference data point was discarded so that only the number of data points defined by eq (3) was used to determine  $\alpha$ . The data point discarded was that farthest from the current baseline point as determined by the maximum distance  $d_j$  determined by the following formula:

$$d_j = \sqrt{\sum_{i=1}^p (x_{i,j} - x_{i,new})^2}, \quad (4)$$

TABLE 2—MESH REFINEMENT STUDY RESULTS

Number of Element Rings	Number of Nodes	Radial Volume Difference (mm <sup>3</sup> )	Longitudinal Volume Difference (mm <sup>3</sup> )	Total Volume Difference (mm <sup>3</sup> )	Approximate (66 MHz 486) Runtime (min)
1	32	357	92	449	2
2	103	290	82	372	4
3	214	205	84	289	11
4	365	203	85	288	25
5	556	197	85	282	53
6	787	192	85	277	92

where  $x_{i,new}$  are the design variable coordinates of the new baseline point (as determined by the optimizer in the previous iteration) and  $x_{i,j}$  represent the percentage changes of the  $j$ th data point used to define the previous response surface. Retaining the volume difference data points nearest to the new baseline point provides the best possible description of the response surface in the direction that the iterative process is moving. Note that only one new EPIC run is required for each response surface update.

An algorithm was devised to determine design variable move constraints for the optimizer. Move constraints prevented the optimizer from extrapolating a solution too far from the defined response surface. Large extrapolations can be inaccurate, which can cause the optimization process to diverge. This algorithm determined the move constraints based on how the response surface was initially defined and how the actual  $V/V_0$  (from an EPIC analysis) compared with the  $V/V_0$  predicted by eq (2).

As stated above, the response surface was initially defined limiting the design variables to changes of  $\pm 10$  percent. Then, for the first iteration, the design variable changes were constrained to remain in the range of  $\pm 20$  percent. This represented a 10-percent extrapolation beyond the data points used to define the response surface. In subsequent iterations, the percentage change limits were halved when the percentage error in the predicted volume difference [given by eq (2)], as compared with the results of an actual EPIC calculation, exceeded the move constraints of that iteration. This scheme ensured that the response surface was kept valid and allowed for zooming in on the optimum in a numerically stable and efficient fashion.

The material constants finally used to produce the smallest possible volume difference are assumed to be the best material constants obtainable from the Taylor test.

### Test Case 1—Coefficient Optimization Starting from Nominal Initial Values

Initially, the nominal Johnson-Cook material strength constants provided by the material library within EPIC for OFHC copper were used to start the optimization process. These constants were given earlier in Table 1. Although this set of constants was obtained specifically for this material, the manufacturing history can cause the material characteristics of OFHC copper to vary somewhat. These nominal constants were expected to provide reasonably accurate results when compared to the Taylor test results. Figure 3 compares the profile of the EPIC solution obtained using these nominal constants with the experimental profile of the primary specimen (described previously) launched at 214 m/s. Here, the EPIC solution can be seen to match the curvature changes

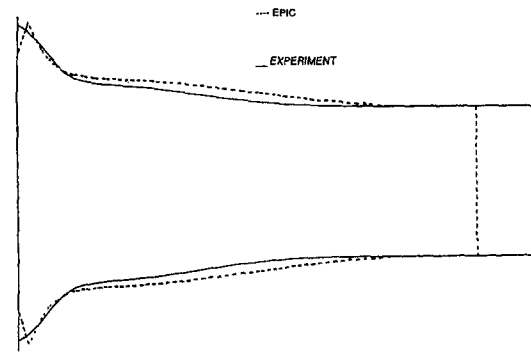


Fig. 3—Comparison of measured and calculated Taylor specimen profiles using nominal strength model constants

in the profile of the measured specimen. However, there is a considerable difference in the overall length. The volume differences corresponding to these nominal constants were calculated to be 408 mm<sup>3</sup>, 259 mm<sup>3</sup> and 149 mm<sup>3</sup> for the total, radial and longitudinal differences, respectively. To get a sense of the magnitude of this error, the relative volume difference can be calculated by dividing the total volume difference by the final deformed specimen volume of 1765 mm<sup>3</sup>. The relative volume difference was 23.1 percent for this initial model based on nominal values for the material constants.

Following the methodology described above, 20 EPIC runs were made to initially define the response surface. The initial array of  $\alpha$  was then calculated, and the iterative process was performed to minimize  $V/V_0$  using the above design variable move constraint algorithm. It was necessary to perform six iterations to approach a local minimum as indicated in Table 3. The third iteration produced a volume difference greater than the preceding iteration. This indicates that the response surface was inaccurate in the region of interest for this iteration. The deformed physical specimen and the EPIC model output using the constants obtained from the sixth iteration are shown in Fig. 4. The final relative volume difference was 4.5 percent.

### Test Case 2—Coefficient Optimization Starting from Calibrated Initial Values

To define a starting point independent of the nominal values described in the previous section, a new set of constants was calculated to accurately match the results of a quasi-static tension test of OFHC copper. Known values for the variables  $\epsilon$  (0.2-percent offset),  $\dot{\epsilon}^*$  ( $= 1.667 \text{ E-4}$ ) and  $T^*$  ( $= 0$ ) were inserted into the strength model, and then material constants  $A$  and  $B$  were adjusted proportionally such that the

TABLE 3—ITERATION HISTORY FOR MATERIAL CONSTANTS OPTIMIZATION STARTING FROM NOMINAL VALUES

Iteration	A (MPa)	B (MPa)	<i>n</i>	<i>C</i>	<i>m</i>	Volume Difference (mm <sup>3</sup> )
0	89.6	291.6	0.3100	0.02500	1.0900	408
1	107.6	350.0	0.2480	0.02875	0.8720	152
2	102.4	385.0	0.2232	0.02587	0.7848	100
3	107.5	404.2	0.2120	0.02716	0.8240	103
4	104.9	394.7	0.2176	0.02652	0.8044	85
5	106.2	389.7	0.2149	0.02685	0.7943	80
6	105.6	392.1	0.2136	0.02702	0.7893	80

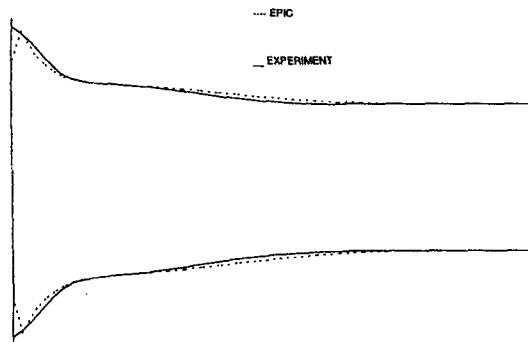


Fig. 4—Comparison of measured and calculated Taylor specimen profiles using calibrated strength model constants

yield strength obtained from the tension test (306 MPa) was matched by eq (1). These values were  $A = 258$  MPa and  $B = 840$  MPa. It was observed that  $n$ ,  $C$  and  $m$  do not change significantly for various alloys of the same metal. Accordingly, these constants were left unchanged from their nominal values (Table 1). Using these calibrated material constants in an EPIC run produced an initial relative volume difference of 29.3 percent.

From this baseline point,  $V/V_0$  was minimized using eight iterations of the response surface approach. The optimum had a relative volume difference of 2.8 percent, somewhat less than that of the first analysis. The optimal coefficients obtained for this analysis were  $A = 132$  MPa,  $B = 430$  MPa,  $n = 0.1786$ ,  $C = 0.01280$  and  $m = 0.5581$ .

#### Averaged Material Constants

It was initially thought that the two apparently different sets of optimized constants obtained here might indicate a uniqueness problem. Ideally, a valid strength model should produce a single local minimum point in the volume difference response surface. A test was devised to determine if the two sets of constants were independent of each other or if they actually described essentially the same local minimum on the response surface. It was assumed that if the two sets of constants represented different local minimum points, then their mean values would produce a set of constants that would be meaningless and would yield inaccurate results when used to simulate the Taylor test. The mean values of the two previously obtained sets of constants were  $A = 118.9$  MPa,  $B = 411.2$  MPa,  $n = 0.1961$ ,  $C = 0.01991$  and  $m = 0.6737$ . These constants were used for an EPIC run that yielded a relative volume difference of only 2.3 percent. These averaged constants actually produced more accurate results than the previously determined sets of constants. Because the mean set

of material constants produced accurate results, it was assumed that the first two sets of constants actually described the same local minimum on the volume difference response surface. Apparently, the response surface is relatively flat in the vicinity of the local minimum.

#### Test Case 3—Constrained Coefficient Optimization

Ideally, one set of material constants should allow for accurate strength predictions over all possible plastic strains, strain rates and temperatures. However, comprehensiveness appears to be too much to ask of simple strength models. This may not necessarily be a problem, since the material constants can be fit for various regimes of interest for the material.

In the second test case, the initial strength model constants were adjusted to match the quasi-static yield strength obtained from a tension test. As the optimization proceeded, the constants were altered to the point where the strength calculated from the model could no longer reproduce the quasi-static yield strength. To determine if the constants for the Johnson-Cook model could be forced to provide for the correct quasi-static yield strength and still give accurate Taylor test results, a third optimization run was conducted with  $A$ ,  $B$ ,  $n$  and  $C$  constrained to change such that the quasi-static yield stress was always correctly predicted. This was easy to impose with the spreadsheet function. This third material constant optimization test case was started from the same set of constants as that of the second optimization test case.

The final, optimal, relative volume difference for this third test case was 9.7 percent. The measured and calculated profiles are compared in Fig. 5. Although the fit of Fig. 5 was not as good as those obtained from the first two test cases, the fit was quite remarkable considering that the constants used to generate the numerical results are forced to span strain rates ranging over eight orders of magnitude.

#### Material Constants Validation

Previously, three sets of material constants were obtained to simulate a Taylor impact test using the primary OFHC copper cylinder (7.87 mm in diameter with a 5:1 aspect ratio) and an impact velocity of 214 m/s. These constants were found to produce reasonably accurate results for this geometry and impact velocity. The accuracy of these material constants was evaluated by simulating six different Taylor tests for which experimental data were available. The first two tests used cylinders having the same diameter and aspect ratio as before, but with higher and lower impact velocities. The next two tests used cylinders of the same diameter and approximately the same impact velocity as before, but having aspect ratios of 3:1 and 10:1. The final two tests used 12.7 mm and

TABLE 4—RESULTS OF THE VALIDATION TESTS

Test	Diameter (mm)	Aspect Ratio	Impact Velocity (m/s)	Relative Volume Difference (%)	
				Mean Constants	Physical Constants
1	7.87	5:1	234	2.9	11.8
2	7.87	5:1	182	3.2	8.8
3	7.87	3:1	210	5.8	14.3
4	7.87	10:1	197	3.0	8.7
5	12.7	7.5:1	195	3.9	13.1
6	4.32	7.5:1	211	3.5	10.6

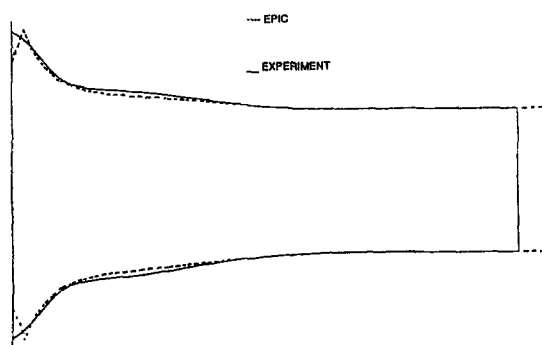


Fig. 5—Comparison of measured and calculated Taylor specimen profiles using constrained strength model constants

4.32 mm diameter cylinders with 7.5:1 aspect ratios. Table 4 lists the characteristics of the six validation tests.

The six validation tests were run using two sets of material constants for each. The first set of constants was the mean of the first two optimization test cases (mean constants). These were used because they represent the most accurate set of constants obtained. The second set of constants (physical constants) was the set found from the third test case. This set was used to determine if material constants with physical meaning (valid for the quasi-static tension test) could be used to accurately simulate other impact conditions. The results of the validation tests are also listed in Table 4.

Although none of the results from the validation tests using the mean constants proved to be as accurate as the relative volume error obtained for the primary cylinder, they were still acceptable. No pattern based on impact velocity, aspect ratio or caliber was found to imply that the mean constants yield more accurate results under one set of conditions as opposed to another. The relative volume differences obtained from the second and fourth validation tests using the physical constants were more accurate than the results of the primary test. However, none of the results obtained with physical constants were comparable to the accuracy obtained using the mean constants.

## Summary

A new methodology was developed for using the Taylor impact test to obtain constants for material strength models. This methodology uses the Taylor specimen's entire deformed geometry and can theoretically be employed to determine all of the constants of any material strength model. This is accomplished by using a second-order polynomial to describe the volume difference between a deformed Taylor test cylinder and a finite element simulation of the test. This polynomial represents a response surface having design variables

that are percentage changes in the constants of the strength model being used. Using a spreadsheet function (such as the Solver tool of Microsoft® Excel®) or some other optimization package, the volume difference can be minimized by changing the design variables to yield a more accurate set of material constants. This is repeated in an iterative scheme, using the newest set of constants as the starting point of each minimization until the volume difference cannot be further reduced. Use of the methodology is illustrated by obtaining material constants for a modified Johnson-Cook model of OFHC copper.

## References

1. Johnson, G.R., "EPIC-3, a Computer Program for Elastic-plastic Impact Calculations in 3 Dimensions," Contract Report BRL-CR-343, Honeywell Inc., Hopkins, MN (1997).
2. Johnson, G.R., "Material Characterization for Warhead Computations," Tactical Missile Warheads, ed. J. Carleone, American Institute of Aeronautics and Astronautics, Washington, DC, 165-197 (1993).
3. Johnson, G.R. and Cook, W.H., "A Constitutive Model and Data for Metals Subjected to Large Strains, High Strain Rates and High Temperatures," Proc. 7th Int. Symp. Ballistics, The Hague, Netherlands (April 1983).
4. Holmquist, T.J. and Johnson, G.R., "Determination of Constants and Comparison of Results for Various Constitutive Models," J. De Physique IV, 1, C3-853-C3-860 (1991).
5. Zerilli, F.J. and Armstrong, R.W., "Dislocation-mechanics-based Constitutive Relations for Material Dynamics Calculations," J. Appl. Phys., 61 (5), 1816-1825 (1987).
6. Follansbee, P.S. and Kocks, U.F., "A Constitutive Description of the Deformation of Copper Based on the Use of Mechanical Threshold Stress as an Internal State Variable," Acta. Metall., 36 (1), 81-93 (1988).
7. Taylor, G.I., "The Use of Flat-ended Projectiles for Determining Dynamic Yield Stress," Proc. Roy. Soc. London, Series A., 194, 289-299 (1948).
8. Lee, E.H. and Tupper, S.J., "Analysis of Plastic Deformation in a Steel Cylinder Striking a Rigid Target," J. Appl. Mech., 21, 63-70 (1954).
9. Hawkyard, J.B., "A Theory for the Mushrooming of Flat-ended Projectiles Impinging on a Flat Rigid Anvil, Using Energy Considerations," Int. J. Mech. Sci., 11, 313-333 (1969).
10. Jones, S.E., Gillis, P.P. and Foster, J.C., Jr., "On the Equation of Motion of the Undeformed Section of a Taylor Impact Specimen," J. Appl. Phys., 61, 499-502 (1987).
11. Mauldin, P.J., Davidson, R.F. and Henninger, R.J., "Implementation and Assessment of the Mechanical-threshold-stress Model Using the EPIC2 and PINON Computer Codes," Contract Report LA-11895-MS, Los Alamos National Laboratory, Los Alamos, NM (1990).
12. Hammerberg, J.E., Preston, D.L. and Wallace, D.C., "A New Model of Rate Dependent Elastic-plastic Flow," APS 1991 Topical Conf. Shock Compression of Condensed Matter, Williamsburg, VA (1991).
13. Pazzienza, G., Pezzica, G. and Vignolo, G.M., "Determination of the Armstrong-Zerilli Constitutive Model for AISI 316 H Stainless Steel and Application to Cylinder Impact Tests," 7th Dymat Technical Conf., St. Louis, MO (1992).
14. Johnson, G.R. and Holmquist, T.J., "Evaluation of Cylinder-impact Test Data for Constitutive Model Constants," J. Appl. Phys., 64, 3901-3910 (1988).
15. Allen, D.J., "Use of the Taylor Impact Test to Determine Constants for Material Strength Models," MS thesis, University of Alabama, Tuscaloosa (1995).